https://doi.org/10.5194/hess-2023-229
Preprint. Discussion started: 27 November 2023
© Author(s) 2023. CC BY 4.0 License.

Hydrology and Earth System Sciences
Discussions

Technical note: Wellbore water volume computation of tracer test in numerical modelling in a confined aquifer

Yiqun Gan[a, b] and Quanrong Wang[a, b*]

[a]School of Environmental Studies, China University of Geosciences, Wuhan, Hubei 430074, PR China

[b]Key Laboratory of Groundwater Quality and Health of Ministry of Education, China University of Geosciences, Wuhan 430074, China

Correspondence to: Quanrong Wang (wangqr@cug.edu.cn)

Abstract.

Computation of the water volume in the operational wellbore is a critical for numerical modeling of dissolved substances movement during aquifer remediation or tracer test in a confined aquifer, which affects the concentration variation, especially in the early stage of the test. In a confined aquifer, the water level is higher than the aquifer top elevation, and the water volume of the aquifer is controlled by the volume of aquifer when ignoring the water compressibility. We found that the wellbore was also treated to be confined in the numerical modeling of tracer test in a wellbore-confined aquifer system. As a result, the wellbore water volume is computed by the aquifer thickness instead of wellbore water level, such as the software package of MODFLOW/MT3DMS, which is incorrect. Actually, the wellbore is open to the air in the confined aquifer, and it is unconfined. In this study, a 3D reactive transport model is revised based on the mass balance in a well-aquifer system with special attention given to the wellbore water volume. The accuracy of new model is tested against benchmark analytical solutions. The results show that previous models may cause significant errors in both aquifer and wellbore for tests with injection wells. As for tests with extraction wells, the error is obvious in the wellbore, but not in the aquifer. Specifically, previous models overestimate the concentration of solute in both aquifer and wellbore under the injection well test case, while it underestimates the concentration in the extraction well test case. The revised model could increase the accuracy of reactive transport modeling in aquifer remediation through the wellbore.

Keywords: Wellbore; Radial dispersion; Finite-difference scheme; Mixing processes

https://doi.org/10.5194/hess-2023-229
Preprint. Discussion started: 27 November 2023
© Author(s) 2023. CC BY 4.0 License.

Hydrology and Earth System Sciences
Discussions

1 Introduction

Wellbore is only way used to obtain the physical and chemical parameters of an actual confined aquifer during aquifer remediation or tracer test (Anderson et al., 2015; El-Kadi, 1988). For instance, the chemicals are injected or extracted through it during the *in-situ* tracer test, and then the parameters, like dispersivity, chemical reaction rate, etc, are estimated by the mathematical models through best fitting the time series concentration observed during tracer test. Therefore, the robustness of the mathematical models of tracer test is critical for the accuracy of parameter estimation.

According to the treatment of solute transport in wellbore, the mathematical models could be classified into two types, which will be reviewed in Section 2. The first type of mathematical models is that the wellbore is treated as the inner boundary condition of reactive transport in the aquifer (named as IBC model), and they are preferred by the analytical solutions. The second type of mathematical models is that the well is treated as a source or sink (named as SS model), and they are preferred by the numerical solutions, due to the complexity of hydrogeological conditions (like heterogeneity, transiency of flow field).

The SS models of tracer test is composed two parts: solute transport in wellbore and aquifer, as shown in Figure S1 in ***Supplementary Material***. In the confined aquifer, the wellbore is open to the air, and it is unconfined. After a careful review of the literature, we found that previous numerical solutions of two-dimensional (2D) and three-dimensional (3D) SS models of tracer test in the Cartesian coordinate system did not properly treat the mixing processes between original water and tracers entering into the operational wellbore in a confined aquifer. The objectives of this study include: the revisit of the treatment of wellbore storage in mathematical models of reactive transport in a wellbore-aquifer system, the revised

https://doi.org/10.5194/hess-2023-229
Preprint. Discussion started: 27 November 2023
© Author(s) 2023. CC BY 4.0 License.

Hydrology and Earth System Sciences
Discussions

numerical solution of the SS model describing the mixing processes between solute in wellbore during the reactive transport, the validation of the revised model, and the influence of wellbore storage on tests involving an injection or an extraction well.

2. Review of mathematical models of tracer test

2.1 The IBC model of tracer test in confined aquifer

When the wellbore is considered as an inner boundary condition, the wellbore-aquifer system reduces the aquifer system, as the concentration variation of solute in the wellbore is not included in the governing equation (Veling, 2012; Wang and Zhan, 2013), e.g.,

$$\frac{\partial(\theta C^k)}{\partial t} = L_{DSP}(C^k)+L_{ADV}(C^k)+L_{SSM}(C^k) + L_{RCT}(\theta C^k),\ t > 0, \quad (1)$$

$$C^k(r,z,t)|_{r=r_w} = f(z,t),\ t > 0, \quad (2a)$$

$$\text{or } \left[v_r C^k(r,z,t) - \alpha_r|v_r|\frac{\partial C^k(r,z,t)}{\partial r}\right]\Big|_{r=r_w} = v_r f(z,t),\ t > 0, \quad (2b)$$

where C^k is dissolved concentration of species k [ML^{-3}]; k is a positive integral to account for the number of species [dimensionless]; t is time [T]; r is radial distance from the wellbore [L]; z is vertical distance; θ is porosity of the porous medium [dimensionless]; r_w is wellbore radius [L]; α_r and v_r are radial dispersivity [L^{2}T^{-1}] and radial flow velocity [LT^{-1}], respectively; $L_{DSP}(\cdot)$, $L_{ADV}(\cdot)$, $L_{SSM}(\cdot)$, and $L_{RCT}(\cdot)$ are operators for dispersion, advection, other sink/sources excluding the discharge/recharge in the wellbore, and chemical reaction terms, respectively; $f(t)$ represents the concentration variations of solute in the wellbore, which is a function of time. Eq. (1) is the multi-species governing equation of reactive transport. Eqs. (2a) - (2b) are the inner boundary conditions, representing the resident concentration

https://doi.org/10.5194/hess-2023-229
Preprint. Discussion started: 27 November 2023
© Author(s) 2023. CC BY 4.0 License.

Hydrology and Earth System Sciences
Discussions

continuity and the flux concentration continuity at the well-aquifer interface, respectively, while Eq. (2b) is recommended since it could keep mass balance for solute transport in the aquifer. The difference between them could be seen in Schwartz et al. (1999) and Novakowski (1992).

This type of models is generally established in the radial coordinate system, such as Wang and Zhan (2013). This is because the flow field is radial when only one well exists and the regional flow (or ambient flow) is negligibly small. The advantage of the radial coordinate system is that it could simplify the mathematical models from two dimensions into one dimension (Chen, 1985; Chen et al., 2012; Novakowski, 1992) or from three dimensions into two dimensions (Huang et al. 2010; Chen, 2010; Chen et al., 2011), for which elegant analytical models may be developed. As for the 2D radial transport, the operators of $L_{DSP}(\cdot)$, $L_{ADV}(\cdot)$, $L_{SSM}(\cdot)$, and $L_{RCT}(\cdot)$ are

$$L_{DSP}(C^k) = \frac{1}{r}\frac{\partial}{\partial r}\left(rD_{rr}\frac{\partial C^k}{\partial r} + rD_{rz}\frac{\partial C^k}{\partial z}\right) + \frac{\partial}{\partial z}\left(D_{zr}\frac{\partial C^k}{\partial z} + D_{zz}\frac{\partial C^k}{\partial z}\right), \quad (3)$$

$$L_{ADV}(C^k) = v_r\frac{\partial C^k}{\partial r} + v_z\frac{\partial C^k}{\partial z}, \quad (4)$$

$$L_{SSM}(C^k) = q_s C^k, \quad (5)$$

$$L_{RCT}(\theta C^k) = \sum R_n, \quad (6)$$

where D_{rr}, D_{rz}, D_{zr} and D_{zz} are the four components of the dispersion coefficient tensor [L^2T^{-1}], respectively; $\sum R_n$ is chemical reaction term [$ML^{-3}T^{-1}$]; q_s is the volumetric flow rate per unit volume which does not include the pumpage of the wellbore [T^{-1}]; v_z is vertical flow [LT^{-1}].

However, this type of models has two shortcomings. Firstly, the flow field may be not radial in realistic aquifer settings, for instance, when more than one well exists or the regional flow could be ignored. Secondly, Eq. (2a) or Eq. (2b) is used to describe the transport at the well screen, and the

https://doi.org/10.5194/hess-2023-229
Preprint. Discussion started: 27 November 2023
© Author(s) 2023. CC BY 4.0 License.

Hydrology and Earth System Sciences Discussions

concentration in the wellbore is required, e.g. $f(z,t)$, which may be unknown in reality. For the simplicity, many studies have assumed that $f(z,t)$ equaled the concentration of the injected solute inside the wellbore (Chen, 1985; Chen, 2010; Phanikumar and McGuire, 2010; Yeh and Chang, 2013a):

$$f(z,t) = C_{inj}^{k}, \tag{7}$$

where C_{inj}^{k} is the concentration of species k in the injected solute [ML^{-3}]. It is not true, since Eq. (7) does not consider the mixing processes between original water and tracers entering into the operational wellbore, and it overestimates the values of concentration in the wellbore. Novakowski (1992) presented a well model considering the wellbore storage for different scenarios based on the mass balance principle, while the flow field was assumed to be in steady state, and the mixing processes were assumed to be instantaneously completed.

2.2 The SS model of tracer test in confined aquifer

Because of the limitations included in the IBC model, the popular way is to take the wellbore as a source/sink term in the governing equation of reactive transport in the numerical modeling. The governing equation of multi-species reactive transport in the wellbore-aquifer system becomes (Konikow and Grove, 1977; Zheng and Wang, 1999):

$$\frac{\partial(\theta C^{k})}{\partial t} = L_{DSP}(C^{k}) + L_{ADV}(C^{k}) + L_{SSM}(C^{k}) + L_{RCT}(\theta C^{k}) + q_{w}C_{w}^{k},\ t > 0, \tag{8}$$

where q_w is volumetric flow rate per unit volume of aquifer [T^{-1}], and it is positive for injection (when the well acts as a source), and negative for extraction (when the well acts as a sink); C_w^k is the concentration of species k [ML^{-3}], and it is equal to C^k in case of extraction (q_s<0); the operators of $L_{DSP}(\cdot)$ and $L_{ADV}(\cdot)$ are different from ones defined in Eq. (1), for instance,

https://doi.org/10.5194/hess-2023-229
Preprint. Discussion started: 27 November 2023
© Author(s) 2023. CC BY 4.0 License.

Hydrology and Earth System Sciences
Discussions

$$L_{DSP}(C^k) = \frac{\partial}{\partial x_i}\left(\theta D_{ij}\frac{\partial C^k}{\partial x_j}\right), \quad (9)$$

$$L_{ADV}(C^k) = \frac{\partial}{\partial x_i}(\theta v_i C^k), \quad (10)$$

where x_i is distance [L] along the respective Cartesian coordinate axis, i =1, 2, and 3, representing the x, y, and z axes, respectively; D_{ij} is hydrodynamic dispersion coefficient tensor [L^2T^{-1}]; v_i is flow velocity. The definitions of $L_{SSM}(\cdot)$ and $L_{RCT}(\cdot)$ are the same as the ones in Eq. (1). The boundary of Eq. (4) is set far away from the well, where the concentration is equal to the background value.

Different from the first approach in Section 2.1, only the values of q_w and C_w^k are required, which are generally available. Eqs. (8) - (10) have been widely employed for solute transport modeling in many software packages, like MODFLOW/MT3DMS (Zheng and Wang, 1999), FEFLOW (Trefry and Muffels, 2007), TOUGH2 (Pruess et al., 2011), etc.

2.3 Groundwater flow model of tracer test in confined aquifer

Solute transport in the aquifer is mainly controlled by groundwater flow, like dispersion, advection, and reactions, and therefore the mathematical models of groundwater flow have to be solved to obtain the flow velocity or the hydraulic head before solving the models of solute transport. For instance, in the software package of MODFLOW/MT3DMS, the modeling of groundwater flow by MODFLOW is run firstly to produce the spatiotemporal flow filed for modeling solute transport by MT3DMS.

3. Revised finite-difference scheme of the SS models

3.1 Errors of the previous finite-difference scheme of the SS models

https://doi.org/10.5194/hess-2023-229
Preprint. Discussion started: 27 November 2023
© Author(s) 2023. CC BY 4.0 License.

Hydrology and Earth System Sciences
Discussions

The finite-difference scheme of the SS model of tracer test in confined aquifer in the wellbore-aquifer system is (Konikow and Grove, 1977; Zheng and Wang, 1999):

$$MA_{Cell} = NMF_x + NMF_y + NMF_z + NMFSS_{Cell} + NMFR_{Cell}, \quad (11)$$

where

$$NMF_x = -\frac{\partial}{\partial x}(C^k \theta v_x^* \Delta y \Delta z)\Delta x, \quad (12a)$$

$$NMF_y = -\frac{\partial}{\partial y}\left(C^k \theta v_y^* \Delta x \Delta z\right)\Delta y, \quad (12b)$$

$$NMF_z = -\frac{\partial}{\partial z}(C^k \theta v_z^* \Delta x \Delta y)\Delta z, \quad (12c)$$

$$NMFSS_{Cell} = W_s C_s^k \Delta x \Delta y \Delta z, \quad (12d)$$

$$NMFR_{Cell} = \theta \Delta x \Delta y \Delta z \sum R_k, \quad (12e)$$

$$MA_{Cell} = \frac{\partial}{\partial t}(C^k \theta \Delta x \Delta y \Delta z), \quad (12f)$$

where v_x^*, v_y^*, and v_z^* are instantaneous mass velocities [LT^{-1}] along the x, y, and z axes, respectively; W_s is volumetric flux per volume of porous medium [T^{-1}]; C_s^k is the concentration [ML^{-3}] of the solute in the source or sink fluid; Δx, Δy, and Δz are the dimensions [L] of cell along the x, y, and z axes, respectively; MA is mass accumulation rate [MT^{-1}]; NMF is net mass flux [MT^{-1}]; $NMFSS$ is net mass flux by source and sink [MT^{-1}]; $NMFR$ is net mass flux by reactions [MT^{-1}]. When $\Delta x = \Delta y$ and $\Delta x \Delta y = \pi r_w^2$ in the wellbore cell, W_s is injection or extraction rate per volume, and C_s^k is the concentration of the injection or extraction solute.

Eqs. (11) - (12) are used in the WELL package of MT3DMS for modeling reactive transport in the wellbore-aquifer system, which is suitable for the one-cell wellbore model, not for the multi-node well (MNW) model. The MNW model refers to case when the wellbore is vertically discretized into several

https://doi.org/10.5194/hess-2023-229
Preprint. Discussion started: 27 November 2023
© Author(s) 2023. CC BY 4.0 License.

Hydrology and Earth System Sciences
Discussions

cells (e.g., Cell 1, Cell 2, Cell 3, and Cell 4, as shown in Figure 1). In the one-cell wellbore model, the intra-borehole flow is ignored. As for the MNW model, the intra-borehole flow is considered, and there is a special package was developed for both groundwater flow and solute transport based on MODFLOW/MT3DMS, named the MNW package (Konikow and Hornberger, 2006; Konikow et al., 2009).

Eqs. (12a) - (12f) demonstrate that weaknesses of the second type of models is that the wellbore is treats as a part of aquifer, resulting in following two problems. Firstly, the porosity of the wellbore is unity, but it is assumed to the same as the porosity of the surrounding aquifer. Secondly, the term of $\theta\Delta x\Delta y\Delta z$ represents the volume of the water in the cells of the grid system in Figure 1, regardless of aquifer and wellbore. It is constant. Actually, the aquifer cells are different from the wellbore cells in bearing the groundwater. In the confined aquifer cells, the volume of water is not affected by the variation of hydraulic head; however, in the wellbore, the volume of water directly changes with the variation of water level. For simplicity, we will explain it using a 2D reactive transport model.

Figure S1 in ***Supplementary Material*** shows a grid system of 2D reactive transport model in a wellbore-confined aquifer system. According to Eqs. (12a) - (12f), the volume of water in the wellbore is $\theta\Delta x\Delta y\Delta z = B\Delta x\Delta y$, where B is aquifer thickness [L]. Actually, it should be $h_w\Delta x\Delta y$, where h_w is water level [L] in the wellbore.

In the early stage of pumping or extracting phase, the volume of water in the wellbore is critical for the wellbore storage of solute transport. Greater volume results in smaller concentration of solute in the wellbore, due to the mixing processes between the original water in the wellbore and water entering the wellbore or leaving the wellbore.

https://doi.org/10.5194/hess-2023-229
Preprint. Discussion started: 27 November 2023
© Author(s) 2023. CC BY 4.0 License.

Hydrology and Earth System Sciences
Discussions

3.2 Revised finite-difference scheme of the SS models

In this study, Eqs. (8) - (12) are called the "previous models" hereinafter and will be revised by considering the water level variation in a wellbore. Including the wellbore cells in the numerical simulation of flow in a well-aquifer system imposes new challenges. For instance, the simulated aquifer is confined whereas the simulated open wellbore is unconfined. The wellbore may include permeable screen sections and impermeable casings, as shown in Figure 1. Therefore, how to treat the wellbore cells in the numerical models needs to be clarified.

Figure 1 shows the grid system for the general case in the numerical simulation. The well is discretized into several cells, e.g., Cell 1, Cell 2, Cell 3, and Cell 4, and such a well is named as a multi-node well. When the well is discretized into one cell, a multi-node well reduces to a one-cell well. Cell 2, Cell 3, and Cell 4 in Figure 1 represent the permeable screen, which could be treated as point sources/sinks in the model. Cell 1 in Figure 1 represents the impermeable casing, which is the upper most cell above the screen inside wellbore.

As for Cell 1, the lateral boundary is impermeable, which implies that it can only exchange water with Cell 2. Therefore, Cell 1, wellbore above Cell 1, and Cell 2 could be combined into one cell, e.g., a revised Cell 2. The volume of water in this revised Cell 2 is the summation of water in Cell 1, water in wellbore above Cell 1, and water in the original Cell 2. Namely, the volume of water in this revised cell is $\Delta x \Delta y B_{Cell2,w}$, where $B_{Cell2,w} = h_w - z_{Cell2,bot}$; $z_{Cell2,bot}$ is the vertical coordinate of the bottom of Cell 2; h_w is water level of the wellbore. For a confined aquifer, one has $B_{Cell2,w} > \Delta z_{Cell2,w}$, where $\Delta z_{Cell2,w}$ represents the vertical dimension of Cell 2. The validity of such treatment will be investigated in Section 4.2.

https://doi.org/10.5194/hess-2023-229
Preprint. Discussion started: 27 November 2023
© Author(s) 2023. CC BY 4.0 License.

Hydrology and Earth System Sciences
Discussions

Therefore, the mass balance for the revised Cell 2 should be

$$MA_{Cell2} = \frac{\partial}{\partial t}\left(C^k \Delta x \Delta y B_{Cell2,w}\right), \quad (13)$$

and Eq. (12d) becomes

$$NMFSS_{Cell} = W_s C_s^k \Delta x \Delta y B_{Cell2,w}. \quad (14)$$

Since the porosity of the revised Cell 2 is unity, $NMFR_{Cell}$ in Eq. (11) becomes

$$NMFR_{Cell} = \Delta x \Delta y B_{Cell2,w} \sum R_k. \quad (15)$$

The other terms of the revised Cell 2 in Eq. (11) are the same as their counterparts in Eqs. (12a) - (12f). As for other wellbore cells, the mass balance equations are the same as ones in Eq. (11), except that porosity is set as unity. As for aquifer cells, the mass balance equations are the same as Eq. (11).

Similar to MODFLOW/MT3DMS, the finite-difference method will be employed to solve Eq. (8). The code of MT3DMS will be revised to accommodate above special treatments of the wellbore cells (particularly the revised Cell 2 in Figure 2) in this study. The flow field is computed by MODFLOW. The changes of the original MT3DMS code are explained in Sections 1 and 2 of Supplementary Materials.

As for a one-cell wellbore (when the well is discretized into a cell), solute transport in the well could be similarly treated by equations used in the revised Cell 2.

3.3 Transport models in the wellbore

In actual applications, the flow field is complex for either an injection well or an extraction well, as shown in the laboratory-controlled experiment of Wang et al. (2018), due to turbulent flow caused by the injection/extraction apparatus (usually a pipe) with a smaller diameter than that of the wellbore itself. Different from transport in porous media, the mechanism of solute transport in the wellbore is similar to transport in surface water bodies (e.g. river). Therefore, diffusion effect and advection are considered for

https://doi.org/10.5194/hess-2023-229
Preprint. Discussion started: 27 November 2023
© Author(s) 2023. CC BY 4.0 License.

Hydrology and Earth System Sciences Discussions

solute transport in the wellbore, while mechanical dispersion is absent (because there is no porous media inside the wellbore). In this study, the MNW model (Konikow and Hornberger, 2006) is used to describe the groundwater flow and solute transport in the wellbore, which is based on MODFLOW/MT3DMS.

4. Accuracy of the revised finite-difference scheme of the SS models

To test the accuracy of the new model of this study, a proven analytical solution will be desirable to serve as the benchmark of comparison. Unfortunately, it seems not easy to derive a general-purpose analytical solution that can accommodate many realistic field conditions, such as flow transiency, etc. It is also necessary to test the new model with the analytical solution considering the actual well construction, such as skin effect. However, the available analytical solutions of the two-region model have not considered the wellbore storage. For instance, Chen et al. (2012) assumed that $f(z,t)$ in Eq. (2a) was constant and independent of location and time, and was equal to the concentration of the injected solute. Therefore, we will employ the analytical solution of an injection test by Novakowski (1992), who considered the wellbore storage.

Figures 2a and 2b show the comparison of the breakthrough curves (BTCs) by the analytical and numerical methods in the wellbore, where the vertical axis represents the relative (or normalized) concentration C/C_0, and C_0 is the constant concentration of the injected solute. The legend of "ANA" represents the analytical solutions. The parameters used in this case are as follows: The aquifer dimensions are 100 m× 100 m × 6 m; the horizontal hydraulic conductivity is 10 m/day; the horizontal anisotropy is 1.0, where the horizontal anisotropy is the ratio between the two horizontal principal components of the hydraulic conductivity; the injection flow rate is 20 m^3/day; the porosity is 0.3; the

https://doi.org/10.5194/hess-2023-229
Preprint. Discussion started: 27 November 2023
© Author(s) 2023. CC BY 4.0 License.

Hydrology and Earth System Sciences
Discussions

longitudinal dispersivity is 0.5 m; the ratio of horizontal transverse dispersivity to longitudinal dispersivity is 0.1; the ratio of vertical transverse dispersivity to longitudinal dispersivity is 0.01. As the well radius is always constant, three sets of initial conditions of the hydraulic head are employed to test the influence of water level on the wellbore storage: h_0 =6 m, h_0 =30 m, and h_0 =60 m. A greater initial head implies a greater water level in the wellbore. Since the depth of wellbore might be greater than 100 m, sometime 1000 m for a deep confined aquifer, the maximum value of 60 m for h_0 is not unusual for the initial hydraulic head. As the flow is assumed to be steady state, the information of the specific yield and the specific storage is not needed. The spatial discretization is $\Delta x = 0.4$ m, $\Delta y = 0.4$ m, and Δz=6 m. The aquifer is vertically discretized into one layer. This is because the flow direction is radially horizontal for a well fully penetrating a homogeneous aquifer. The steady-state drawdown in the wellbore is set as -0.346 m for all cases.

A point to note is that wellbore is a cylinder in the analytical solution, while it is approximated as a cuboid in the numerical solution by MODFLOW/MT3DMS. To ensure the same water volume used in both analytical and numerical solutions, the well radius (r_w) of the analytical solution is calculated by the following equation:

$$r_w = \sqrt{\frac{\Delta x \Delta y}{\pi}}. \quad (16)$$

Figure 2a shows that the numerical solution by previous MT3DMS code is independent of the water level in the wellbore, which is close to the analytical solution when the initial water level inside the wellbore is 6 m (the same as the aquifer thickness). However, when the initial water level inside the wellbore is substantially different from the aquifer thickness of 6 m, considerable discrepancies can be seen between the analytical and numerical solutions. This figure demonstrates that the previous models of Eqs. (8) -

https://doi.org/10.5194/hess-2023-229
Preprint. Discussion started: 27 November 2023
© Author(s) 2023. CC BY 4.0 License.

Hydrology and Earth System Sciences
Discussions

(12) may cause significant errors in describing solute transport around a wellbore when the initial water level inside the wellbore is considerably different from the aquifer thickness. Figure 2b shows the comparison between the analytical solution and numerical solution by the revised MT3DMS code of this study, and they match well with each other, with some minor discrepancies (but noticeable). Such minor discrepancies may be caused by two factors. First, the vertical surface area of the screen in the analytical solution (cylinder) is different from that in the numerical solution (cuboid) when the volume of the cuboid well is equal to the volume of the cylinder well. For instance, based on the setting of this study (r_w= 0.226 m, B =6 m, $\Delta x = 0.4$ m), the surface area of a cylinder is $2\pi r_w B$=8.51 m^2, while the vertical surface area of a cuboid is $4\Delta x B$=9.60 m^2. Such a difference in surface area of the screen may generate a minor discrepancy between the analytical and numerical solutions. Second, numerical errors (like numerical dispersion) may not be completely eliminated in the finite-difference solution.

In addition, it is desirable to test the new models using an extraction well test. However, the analytical solution for such a case is not available if the wellbore storage must be taken into consideration. This is an open research problem that will be investigated in the near future.

5. Discussions

In aquifer remediation practices, both injection and extraction wells have been widely employed (Anderson et al., 2015; El-Kadi, 1988). Although the influence of the wellbore storage has been investigated for an injection well test case in Section 4, an important assumption should not be overlooked: the flow is under steady-state condition, which might not always be satisfied in actual applications. In this section, the wellbore storage of solute transport around both injection and extraction wells under transient

https://doi.org/10.5194/hess-2023-229
Preprint. Discussion started: 27 November 2023
© Author(s) 2023. CC BY 4.0 License.

Hydrology and Earth System Sciences Discussions

flow condition will be investigated to see how the flow transiency will affect the results obtained from the steady-state assumption.

5.1 The injection test in a homogeneous aquifer

Figure 3 shows the comparison of BTCs between the previous models of Eqs. (8) – (12) and revised models of this study Eqs. (13) – (15) at different vertical locations. The value of specific storage is 0.00001 m^{-1}, and the initial water table is 60 m. The parameters used are the same with ones in Figure 2. The legend of "in aquifer" represents the case that the observed BTCs is 3 m away from the wellbore.

This figure demonstrates that the values of BTCs computed by the previous models are smaller than those by the new model, and the difference between them is obvious in both aquifer and wellbore. It demonstrates that errors caused by Eqs. (8) - (12) are not negligible for the case with an injection well.

5.2 The extraction test in a homogeneous aquifer

Figure 4 shows the comparison of BTCs between the previous models and the revised models of this study around an extraction well. The legend of "in aquifer" represents the case that the observed BTCs is 3 m away from the wellbore. The flow rate is -20 m^3/day where negative sign represents extraction. The initial solute plume is a cuboid. Horizontally, the extraction well is located at the center of the plume cuboid, and the side faces of the plume are 5 m away from the well center. The other parameters are the same with ones in Figure 3. This figure shows that BTCs computed by the new model are above ones by the previous model, due to the wellbore storage considered in the new model. The difference of BTCs between them is obvious in the wellbore, but not in the aquifer. One may find that the wellbore storage is generally not significant for solute transport in the aquifer at locations not too close to the wellbore, e.g.

https://doi.org/10.5194/hess-2023-229
Preprint. Discussion started: 27 November 2023
© Author(s) 2023. CC BY 4.0 License.

Hydrology and Earth System Sciences Discussions

3 m in this study. The reason is that the solute mainly moves toward the well, due to the convergent flow field, and the wellbore storage on the aquifer could be ignored.

Therefore, this figure demonstrates that the errors caused by Eqs. (8) - (12) are generally negligible for reactive transport in the aquifer at locations not too close to the wellbore (such as 3 m), but those errors are not negligible for the wellbore.

5.3 The injection test in a heterogeneous aquifer

Generally, the aquifer homogeneity is a simplification of reality. In this section, the aquifer is assumed to be vertically heterogeneous. The vertical heterogeneity is manifested in multiple layers (i.e. a multi-aquifer system). The dimensions of the multi-aquifer system are assumed to be 32 m in length, 32 m in width, and 20 m in height. It is composed of 7 layers from top to bottom: A coarse sand layer with 3.5 m in thickness (1st layer), a medium sand layer with 2 m in thickness (2nd layer), another coarse sand layer with 3.5 m in thickness (3rd layer), a fine sand layer with 2 m in thickness (4th layer), one more coarse sand layer with 3.5 m in thickness (5th layer), a clay layer with 2 m in thickness (6th layer), and finally a coarse sand layer with 3.5 m in thickness (7th layer), as shown in Figure 5. The well screen starts from z=5.5 m to z=16.5 m. The well screen is open in layers 2 - 6. The injection or extraction point is located at the top of the well screen. The hydraulic conductivities of the coarse sand (layers 1, 3, 5, and 7), the medium sand (layer 2), the fine sand (layer 4) and the clay (layer 6) are 10 m/day, 0.1 m/day, 0.01 m/day, and 0.001 m/day, respectively. The common factors for all 7 layers are a specific storage of 0.0001 m^{-1}, a porosity of 0.3, and a longitudinal dispersivity of 0.5 m.

https://doi.org/10.5194/hess-2023-229
Preprint. Discussion started: 27 November 2023
© Author(s) 2023. CC BY 4.0 License.

Hydrology and Earth System Sciences
Discussions

To set up the numerical simulation, the aquifer is discretized into 40 columns × 40 rows × 7 layers. The horizontal discretization is uniform, e.g. $\Delta x = 0.8$ m, and $\Delta y = 0.8$ m, while the vertical discretization matches the layer thickness.

Figures 6A and 6B show the comparison of BTCs between the previous model and the new models of this study. The injection well is located at the aquifer center with a flow rate of 20 m^3/day. Legends of "z=15 m", "z=12.75 m", "z=10 m", and "z=7.25 m" represent the observed locations at 2nd layer (the medium sand layer), 3rd layer (the second coarse sand layer), 4th layer (the fine sand layer), and 5th layer (the third coarse sand layer), respectively, as shown in Figure 5. Figure 6A shows that the solute concentration obtained by the new models is smaller than that by the previous models, implying that the previous models overestimate the solute concentration in the wellbore. This is because Eqs. (8) – (12) underestimate the water volume in the wellbore. Figure 6B shows the comparison of BTCs in the aquifer, and the legends are the same with ones in Figure 6A. One may find that BTCs computed by the new models are lower than BTCs generated by the previous models, and the reason is the same with one in Figure 6A. Additionally, the values of BTCs at *z*=12.75 m and *z*=7.25 m are greater than those at *z*=15 m and *z*=10 m. This is because the locations of *z*=12.75 m and *z*=7.25 m are in the coarse sand layer, whose higher permeability makes solute transport much easier and faster.

6. Summary and conclusions

Solute transport in a well-aquifer system has attracted the attention of scholars in hydrogeology and environmental science during the past few decades. Due to the complexity of the flow field, numerical modeling has been widely used to study the fate and transport of contaminates in the subsurface through

https://doi.org/10.5194/hess-2023-229
Preprint. Discussion started: 27 November 2023
© Author(s) 2023. CC BY 4.0 License.


the interaction of an open borehole and the surrounding aquifer. By revisiting the previous 3D mathematical model of reactive transport in the Cartesian coordinate system, we found that it could not properly describe the wellbore storage in the confined aquifer. In this study, a revised model is developed based on the mass balance principle in a well-confined aquifer system. The conclusions are summarized as follows:

(1) A revised 3D model of reactive transport is proposed and tested against the analytical solutions, and it is much better than the previous models in describing the wellbore storage for a well penetrating a confined aquifer.

(2) For the injection well test case, the previous models of reactive transport may cause errors, which are considerable in both aquifer and wellbore. For the extraction well test case, such errors are obvious in the wellbore, but not in the aquifer.

(3) The previous models overestimate the solute concentration in the injection well test case, while underestimate the concentration in the extraction well test case.

https://doi.org/10.5194/hess-2023-229
Preprint. Discussion started: 27 November 2023
© Author(s) 2023. CC BY 4.0 License.


Code and data availability: The code/datasets used and/or analysed during the current study are available from the corresponding author upon reasonable request.

Author contributions: Methodology, derivation, code, and formal analysis, writing original draft: YG. Conceptualization, writing original draft, writing-review and editing, and supervision: QW.

Competing interests: The contact author has declared that neither they nor their co-authors have any competing interests.

Acknowledgments

This research was partially supported by Programs of Natural Science Foundation of China (No. 41972250), and Innovative Research Groups of the National Nature Science Foundation of China (No. 41521001).

References

Anderson, M. P., Woessner, W. W., and Hunt, R. J.: Applied groundwater modeling: simulation of flow and advective transport, Academic press2015.

Chen, C. S.: Analytical and approximate solutions to radial dispersion from an injection well to a geological unit with simultaneous diffusion Into adjacent strata, Water Resources Research, 21(8), 1069-1076, https://doi.org/10.1029/WR021i008p01069, 1985.

https://doi.org/10.5194/hess-2023-229
Preprint. Discussion started: 27 November 2023
© Author(s) 2023. CC BY 4.0 License.


Chen, J.-S., Liu, Y.-H., Liang, C.-P., Liu, C.-W., and Lin, C.-W.: Exact analytical solutions for two-dimensional advection–dispersion equation in cylindrical coordinates subject to third-type inlet boundary condition, Advances in Water Resources, 34(3), 365-374, https://doi.org/10.1016/j.advwatres.2010.12.008, 2011.

Chen, J. S.: Analytical model for fully three-dimensional radial dispersion in a finite-thickness aquifer, Hydrol. Process., 24(7), 934-945, https://doi.org/10.1002/hyp.7541, 2010.

Chen, Y. J., Yeh, H. D., and Chang, K. J.: A mathematical solution and analysis of contaminant transport in a radial two-zone confined aquifer, Journal of Contaminant Hydrology, 138-139(2012), 75-82, https://doi.org/10.1016/j.jconhyd.2012.06.006, 2012.

El-Kadi, A. L.: Applying the USGS Mass-Transport Model (MOC) to Remedial Actions by Recovery Wells, Groundwater, 26(3), 281-288, https://doi.org/10.1111/j.1745-6584.1988.tb00391.x, 1988.

Konikow, L. F. and Grove, D. B.: Derivation of equations describing solute transport in ground water, US Geological Survey, Water Resources Division, https://doi.org/10.3133/wri7719. 1977.

Konikow, L. F. and Hornberger, G. Z.: Use of the multi-node well (MNW) package when simulating solute transport with the MODFLOW ground-water transport process, US Geological Survey Techniques and Methods, 6-A15, https://doi.org/10.3133/tm6A15. 2006.

Konikow, L. F., Hornberger, G. Z., Halford, K. J., and Hanson, R. T.: Revised multi-node well (MNW2) package for MODFLOW ground-water flow model, US Geological Survey Techniques and Methods, 6-A30, https://doi.org/10.3133/tm6A30. 2009.

https://doi.org/10.5194/hess-2023-229
Preprint. Discussion started: 27 November 2023
© Author(s) 2023. CC BY 4.0 License.


Novakowski, K. S.: The analysis of tracer experiments conducted in divergent radial flow fields, Water resources research, 28(12), 3215-3225, https://doi.org/10.1029/92WR01722. 1992.

Phanikumar, M. S. and McGuire, J. T.: A multi-species reactive transport model to estimate biogeochemical rates based on single-well push-pull test data, Computers & Geosciences, 36(8), 997-1004, https://doi.org/10.1016/j.cageo.2010.04.001, 2010.

Pruess, K., Oldenburg, C., and Moridis, G.: TOUGH2 User's Guide, 2011.

Schwartz, R., McInnes, K., Juo, A., Wilding, L., and Reddell, D.: Boundary effects on solute transport in finite soil columns, Water Resources Research, 35(3), 671-681, https://doi.org/10.1029/1998WR900080. 1999.

Trefry, M. G. and Muffels, C.: Feflow: A finite-element ground water flow and transport modeling tool, Ground Water, 45(5), 525-528, https://doi.org/10.1111/j.1745-6584.2007.00358.x, 2007.

Veling, E. J. M.: Radial transport in a porous medium with Dirichlet, Neumann and Robin-type inhomogeneous boundary values and general initial data: analytical solution and evaluation, J. Eng. Math., 75(2012), 173-189, https://doi.org/10.1007/s10665-011-9509-x, 2012.

Wang, Q. R. and Zhan, H. B.: Radial reactive solute transport in an aquifer-aquitard system, Advances in Water Resources, 61(2013), 51-61, https://doi.org/10.1016/j.advwatres.2013.08.013, 2013.

Yeh, H. D. and Chang, Y. C.: Recent advances in modeling of well hydraulics, Advances in Water Resources, 51(2013), 27-51, https://doi.org/10.1016/j.advwatres.2012.03.006. 2013.

Zheng, C. and Wang, P. P.: MT3DMS: a modular three-dimensional multispecies transport model for simulation of advection, dispersion, and chemical reactions of contaminants in groundwater

https://doi.org/10.5194/hess-2023-229
Preprint. Discussion started: 27 November 2023
© Author(s) 2023. CC BY 4.0 License.

Hydrology and Earth System Sciences
Discussions

systems; documentation and user's guide, Alabama Univ University, http://hdl.handle.net/11681/4734 (last access: 11 May 2023). 1999.

https://doi.org/10.5194/hess-2023-229
Preprint. Discussion started: 27 November 2023
© Author(s) 2023. CC BY 4.0 License.

Figure Captions

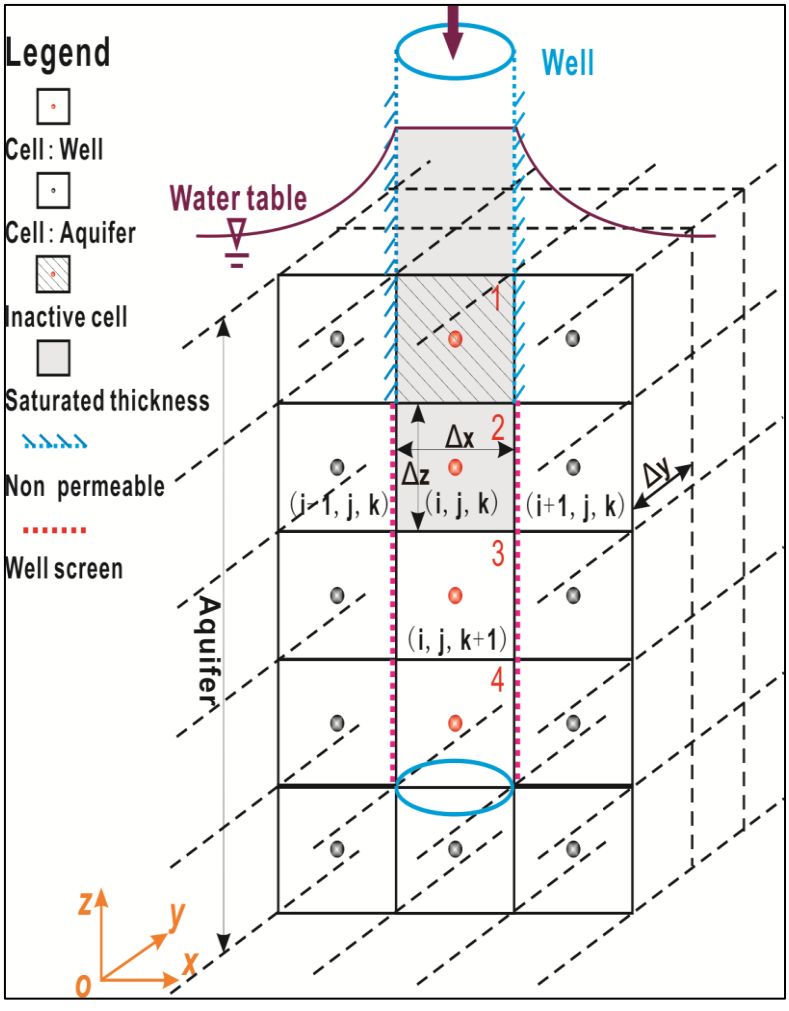

Figure 1. Schematic diagram of the grid system in a numerical simulation of a partially penetrating well. Black lines represent the discretization of the aquifer including the wellbore in the aquifer (e.g. Cell 1, Cell 2, Cell 3, and Cell 4). The part of the wellbore located above the aquifer is not included in the grid system.

https://doi.org/10.5194/hess-2023-229
Preprint. Discussion started: 27 November 2023
© Author(s) 2023. CC BY 4.0 License.

Hydrology and Earth System Sciences
Discussions

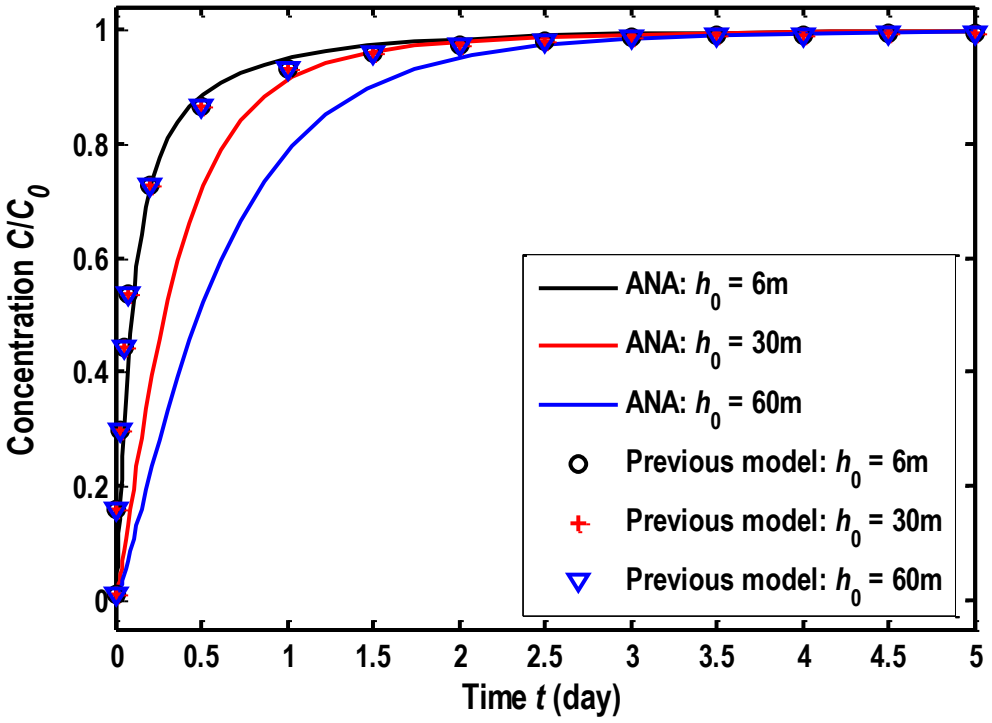

(a) Numerical solutions computed by the previous model

Figure 2. Comparison between BTCs based on analytical and numerical methods in the wellbore under steady state flow conditions. ANA: Analytical solutions.

410

https://doi.org/10.5194/hess-2023-229
Preprint. Discussion started: 27 November 2023
© Author(s) 2023. CC BY 4.0 License.

Hydrology and Earth System Sciences
Discussions

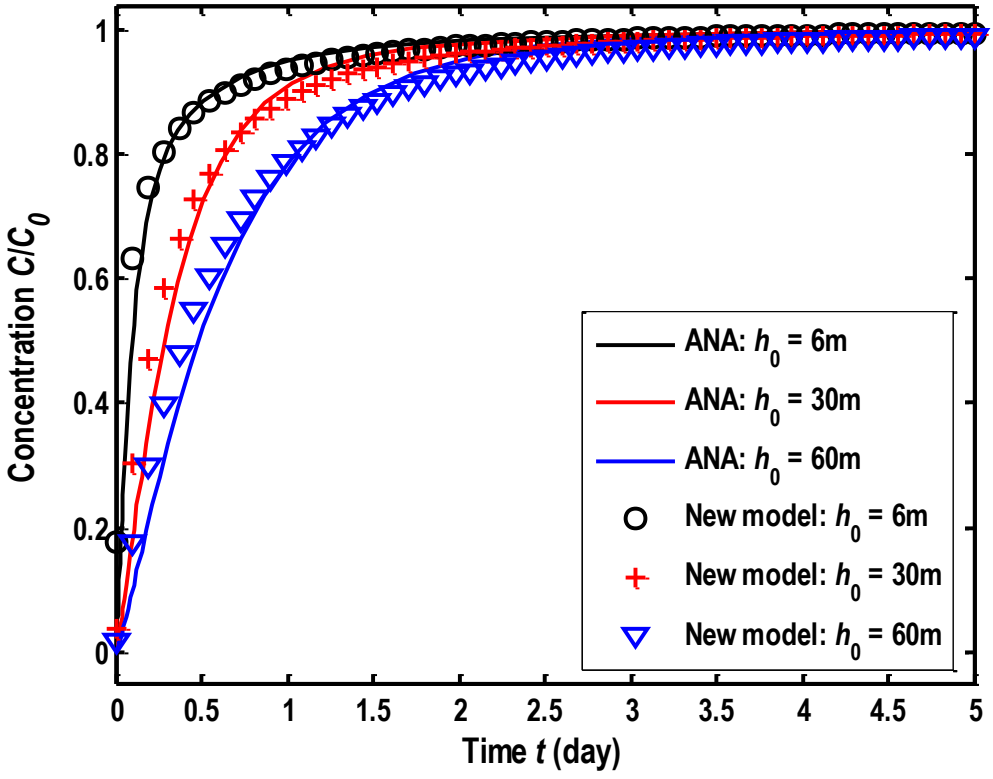

(b) Numerical solutions computed by the revised new model

Figure 2. Comparison between BTCs based on analytical and numerical methods in the wellbore under steady state flow conditions. ANA: Analytical solutions.

415

https://doi.org/10.5194/hess-2023-229
Preprint. Discussion started: 27 November 2023
© Author(s) 2023. CC BY 4.0 License.

Hydrology and Earth System Sciences
Discussions

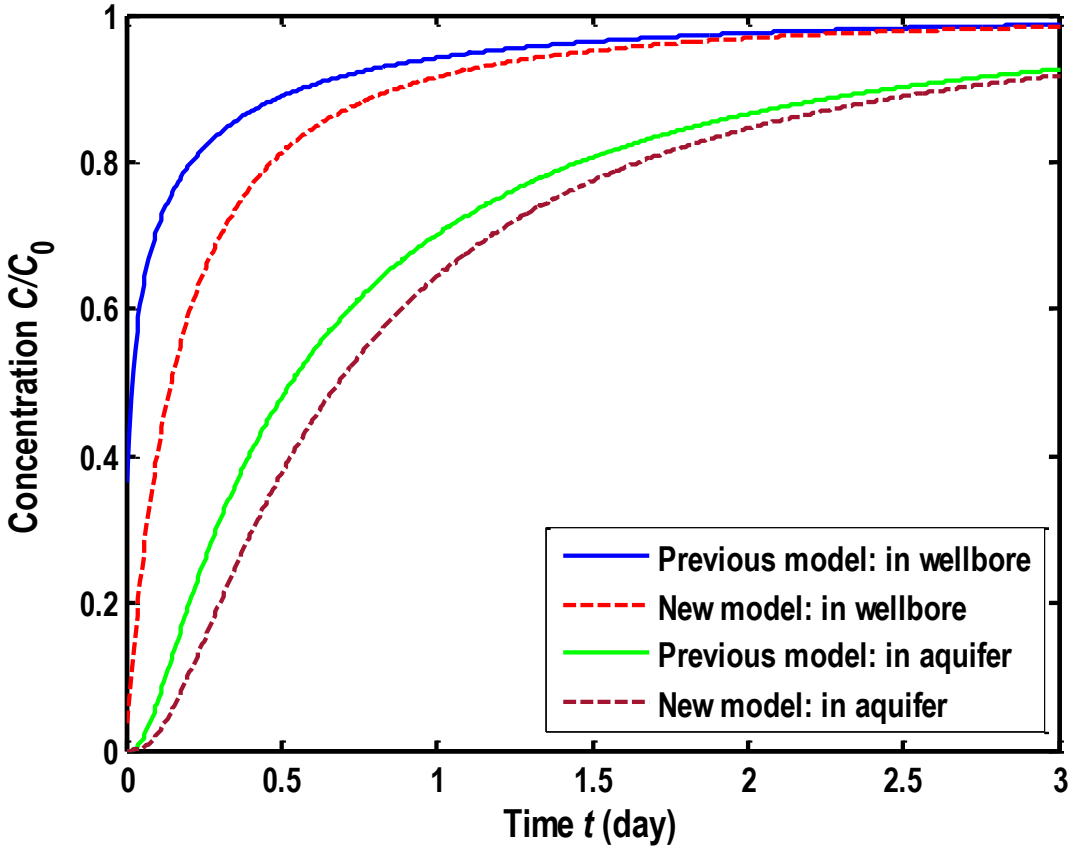

Figure 3. Comparison of BTCs for the injection well test.

https://doi.org/10.5194/hess-2023-229
Preprint. Discussion started: 27 November 2023
© Author(s) 2023. CC BY 4.0 License.

Hydrology and Earth System Sciences
Discussions

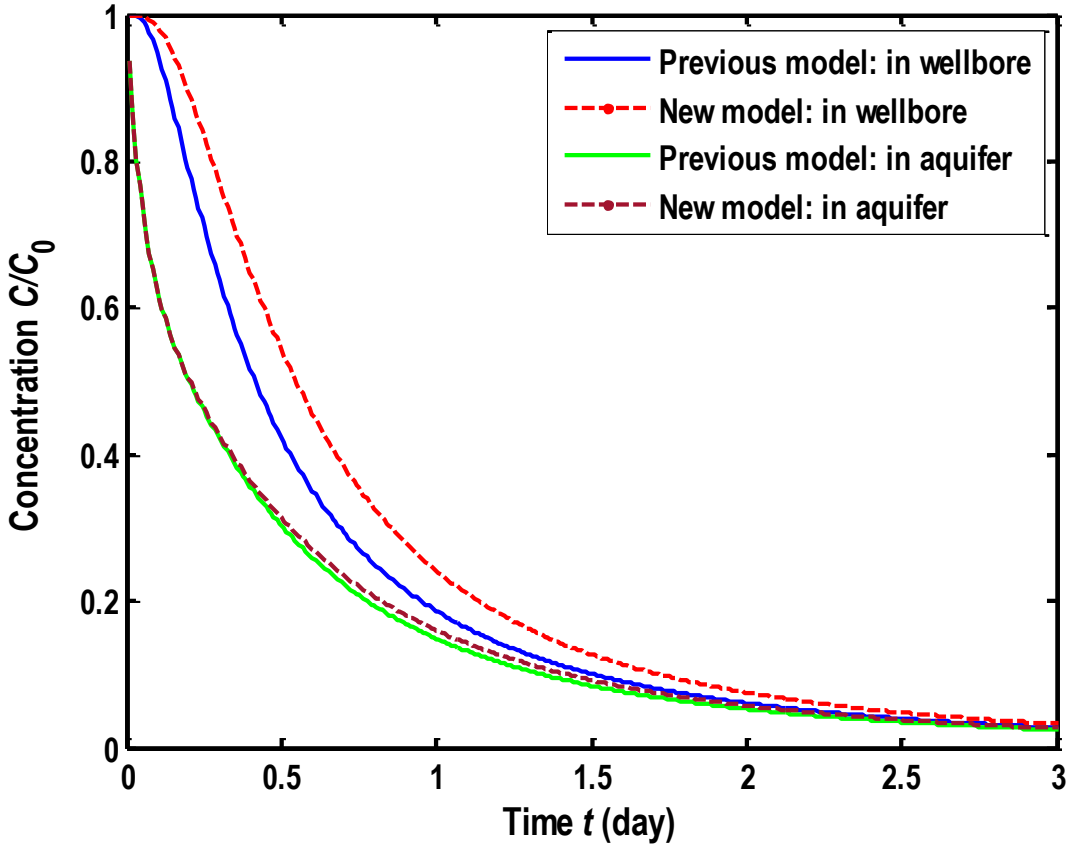

Figure 4. Comparison of BTCs for the extraction well test.

420

https://doi.org/10.5194/hess-2023-229
Preprint. Discussion started: 27 November 2023
© Author(s) 2023. CC BY 4.0 License.

Hydrology and Earth System Sciences
Discussions

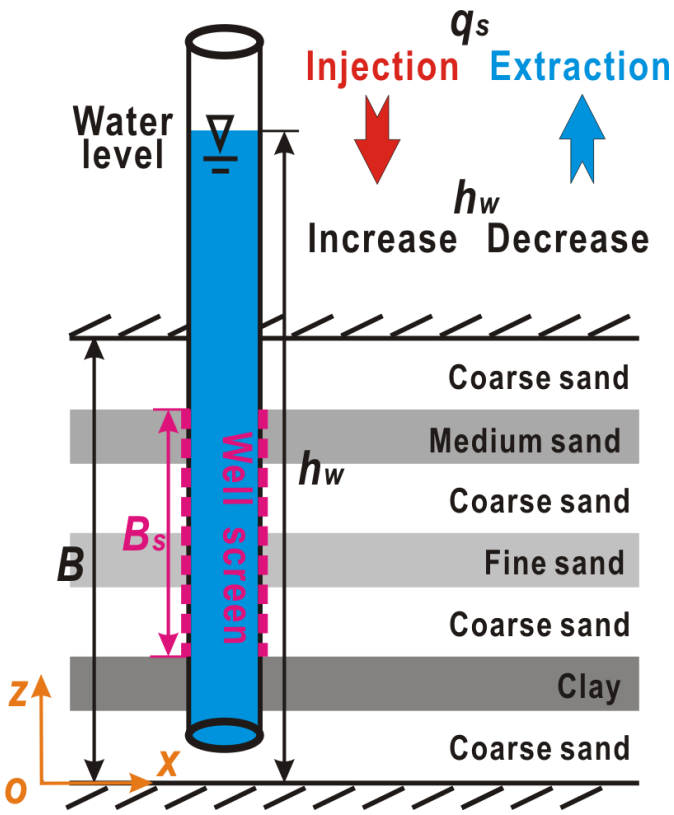

Figure 5. Schematic diagram of the well-aquifer system. The well partially penetrates the stratified aquifer.

https://doi.org/10.5194/hess-2023-229
Preprint. Discussion started: 27 November 2023
© Author(s) 2023. CC BY 4.0 License.

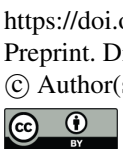

Hydrology and Earth System Sciences
Discussions
Open Access
EGU

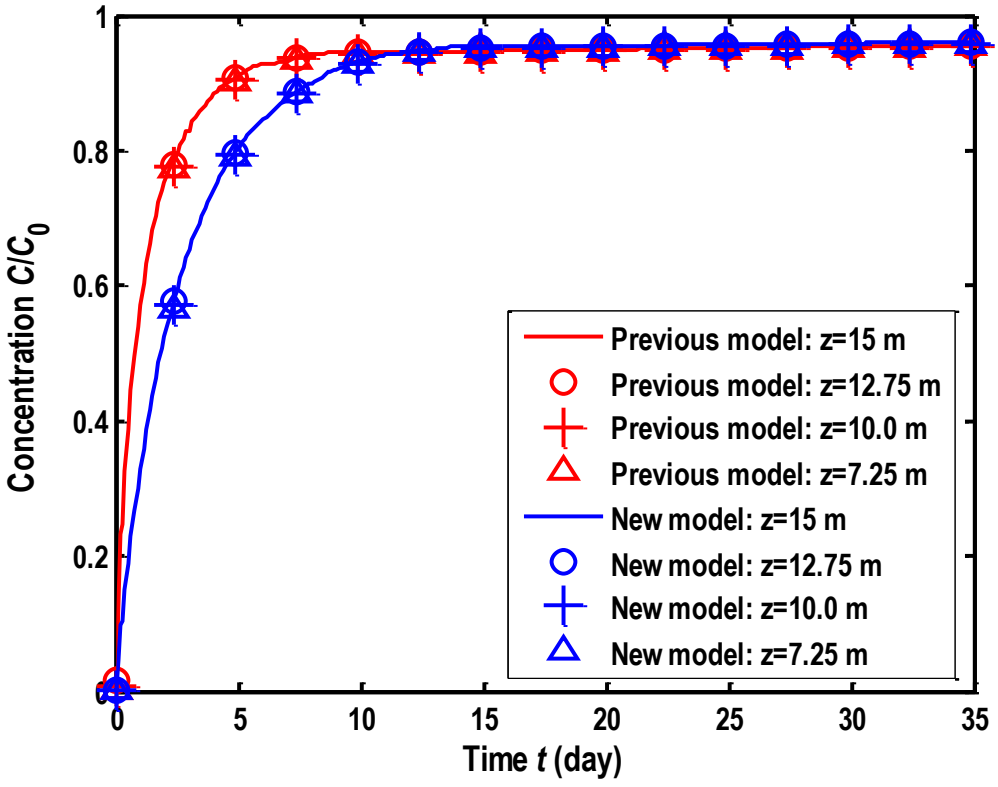

425

(a) BTC in the wellbore

Figure 6. Comparison of BTCs for the two-well test under transient flow conditions.

https://doi.org/10.5194/hess-2023-229
Preprint. Discussion started: 27 November 2023
© Author(s) 2023. CC BY 4.0 License.

Hydrology and Earth System Sciences
Discussions

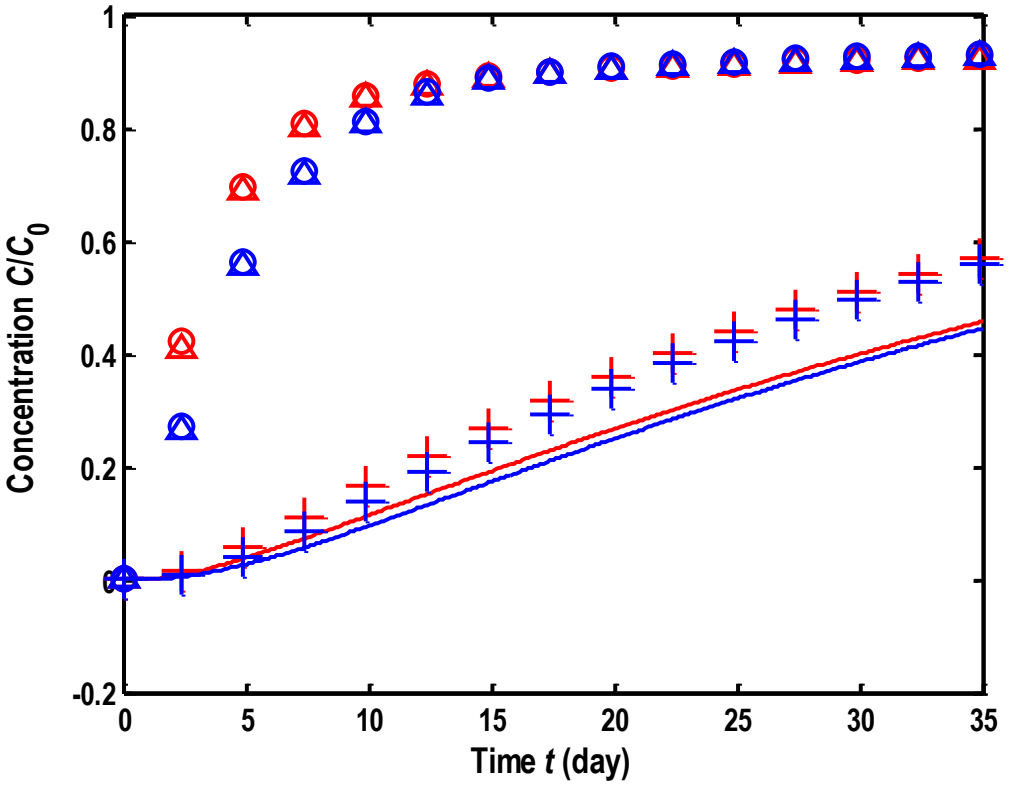

(b) BTC in the aquifer, 1.2 m away from well.

Figure 6. Comparison of BTCs for the two-well test under transient flow conditions.